Kinematics of a Trinal-Branch Space Robotic Manipulator with Redundancy

JIA Qing-xuan[1,2], YE Ping[1], SUN Han-xu[2], SONG Jing-zhou[1]

(1. Institute of Robotic Research, Beijing University of Aeronautics and Astronautics, Beijing 100083, China)

(2. Automation School, Beijing University of Posts and Telecommunications, Beijing 100876, China)

Abstract: This paper presents a trinal-branch space robotic manipulator with redundancy, due to hash application environments, such as in the station. One end-effector of the manipulator can be attached to the base, and other two be controlled to accomplish tasks. The manipulator permits operation of science payload, during periods when astronauts may not be present. In order to provide theoretic basis for kinematics optimization, dynamics optimization and fault-tolerant control, its inverse kinematics is analyzed by using screw theory, and its unified formulation is established. Base on closed-form resolution of spherical wrist, a simplified inverse kinematics is proposed. Computer simulation results demonstrate the validity of the proposed inverse kinematics.

Key words: space robotic manipulators; redundancy; screw theory; inverse kinematics

具有冗余度的三分支空间机器人的运动学分析. 贾庆轩, 叶平, 孙汉旭, 宋荆洲. 中国航空学报(英文版), 2005, 18(4): 378-384.

摘 要: 基于例如空间站等恶劣的应用环境, 研制了一种具有冗余度的三分支空间机器人。该机器人的一个分支的末端可以和基座固联, 另外两个分支可以进行控制来完成各种作业。在宇航员不在的情况下, 该机器人可以代替宇航员对科学实验载荷进行操作。利用旋量理论对机器人的逆运动学进行了分析, 并建立了统一的数学模型给出了其运动学优化、动力学优化以及容错控制的理论基础。基于球腕的封闭解, 提出了一个简单的逆运动学模型。最后, 通过计算机结果演示验证了所提出逆运动学模型的有效性。

关键词: 空间机器人; 冗余度; 旋量理论; 逆运动学

文章编号: 1000-9361(2005)04-0378-07 中图分类号: V260.6; TP242 文献标识码: A

The earliest space robotic manipulators were mostly serial-typed with fixed base, such as Germany's ROTEX[1], Japan's JEMRMS[2], and so on. This kinds of space robotic manipulators have many similarities with traditional industrial robotic manipulators, and all of them have inherent defects that manipulation space is limited.

In order to increase the flexibility, versatility and work space, many mobile space robotic manipulators were proposed by researchers, such as Self-Mobile Space Manipulator (SM) by Xu[3] and Canada's Mobile Servicing System (MSS). The IVA Servicer which has two arms like a man was proposed in NASA's telerobotics program plan. This manipulator can off-load the requirements of intensive astronaut maintenance of science payloads, and permit operation of the payloads during periods when astronauts may not be present[4].

Ren[5] introduced an space robotic manipulator with three branches, which is refered in this paper as trinal-branch space robotic manipulator here, and deduced its inverse kinematics. Besides having the capability of accomplishing all the tasks that the serial-typed robotic manipulators can, the trinal-branch space robotic manipulator can accomplish cooperative manipulation that can not be accomplished with serial-typed robotic manipulators and walk inside or outside the station. Any two

Received date: 2005-03-10; Revision received date: 2005-09-22
Foundation item: "863" Item: National High Technology Foundation in Astronautics(2002AA742030)

branches of the trinal-branch robotic manipulator can buildup a serial-typed robotic manipulator with redundancy. However, when the cooperative manipulation is performed, it acts like a non-redundant robotic manipulator. Therefore, it is inevitable for the trinal-branch robotic manipulator having the defects inherent in non-redundant robotic manipulators which kinematics and dynamics performances can not be optimized, when cooperative manipu-lation is performed.

This paper aims at introducing a trinal-branch space robotic manipulator with redundancy which is flexible and versatile enough to accomplish many complicated tasks in the station. Based on the redundancy, not only its kinematics and dynamics optimizations can be performed, but also the fault-tolerant control controller can be designed to enhance the reliability. This paper also presents the inverse kinematics of the manipulator. Since the configuration of the manipulator is different from those of the traditional serial-typed robotic manipulators, the inverse kinematics is also different.

In the next section, the configuration of the manipulator is presented. Its inverse kinematics is discussed in Section 2. In Section 3, a simplified inverse kinematics model of the manipulator is proposed. Computer simulation and results are presented in Section 4. Section 5 is the conclusion.

1 Configuration of the Trinal-Branch Space Robotic Manipulator

Space robotic manipulators that work in harsh environments are subject to actuator and sensor failures. Repairing the broken actuators and sensors is impossible. Therefore the space robotic manipulators need fault-tolerance ability.

It has long been known that the kinematically redundant robotic manipulators are inherently more dextrous than traditional non-redundant manipulators due to the extra degrees of freedom. This redundancy can be utilized to compensate for one or more failure joints. When some actuator and sensor failures occur, the manipulators still can accomplish tasks if they are properly designed and controlled[6].

This redundancy also can be utilized to optimize the joint torque and joint velocity to reduce the system energy consumation as well as other various performance criterion, including singularity avoidance and obstacle avoidance.

Configuration of the trinal-branch space robotic manipulator with redundancy is shown in Fig. 1.

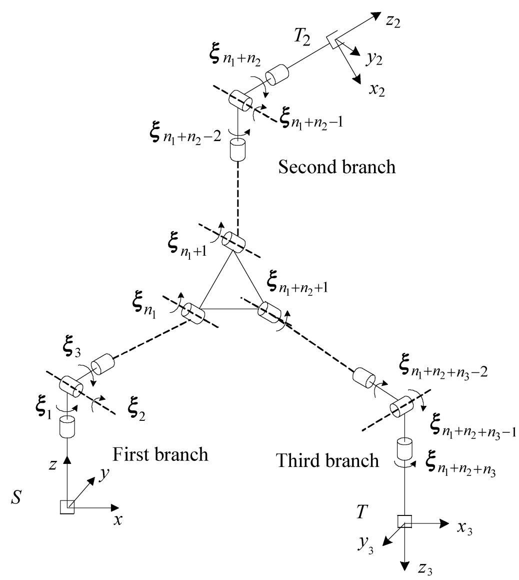

Fig. 1 Configurations of the trinal-branch space robotic manipulator

The manipulator has three branches, which are named first branch, second branch and third branch with n_1, n_2 and n_3 individually. The degree of freedom is $n = n_1 + n_2 + n_3$, and the axis of each revolute joint is shown in Fig. 1.

One end-effector of the three branchs is attached to the station, and the other two are controlled to accomplish various tasks. Therefore, in order to obtain extra degrees of freedom, the manipulator must have at least 13 joints.

2 Kinematics of the Trinal-Branch Space Robotic Manipulators

Previous researches on modeling robotic manipulators' kinematics were mainly based on Denavit-Hartenberg(D-H) parameterization method[7]. However, this method works in a relatively strictly defined coordinate system which increases the complexity of kinematics analysis of robotic manipulator. In this section, the kinematics of the trinal-branch space robotic manipulator is developed based on the Product-of-Exponentials (POE) formula. The POE approach requires only two coordinate frames, one is attached to the base and the other is attached to the end-effector.

2.1 Forward kinematics

The coordinate system of the trinal-branch space robotic manipulator is shown in Fig. 1. Frame S is attached to the base. Frames T_2 and T_3 are attached to the end-effectors of the second branch and the third branch respectively. As shown in Fig. 1, the first branch is attached to the base. $\dot{\xi}_i$ represents the ith joint twist of instantaneous motion, which is a 3 × 3 skew-symmetric matrix relative to S. $\hat{\xi}_i$ can also be written as $\hat{\xi}_i = (\omega_i, v_i) \in \mathbf{R}^6$, named a twist coordinate.

The first and the second branches buildup a serial-typed manipulator, so do the first branch and the third branch, which are named manipulator M_2 and M_3 respectively.

Let $\boldsymbol{g}_{st,2}(0)$ and $\boldsymbol{g}_{st,3}(0) \in \mathbf{R}^{4\times 4}$ represent the initial poses of end-effetor of M_2 and M_3 relative to S respectively. The POE forward kinematics of M_2 and that of M_3 can be expressed as

$$\left.\begin{aligned}\boldsymbol{g}_{st,2}(\theta) &= \prod_{i=1}^{n_1} e^{\xi_i\theta_i} \prod_{j=n_1+1}^{n_1+n_2} e^{\xi_j\theta_j} \boldsymbol{g}_{st,2}(0) \\ \boldsymbol{g}_{st,3}(\theta) &= \prod_{i=1}^{n_1} e^{\xi_i\theta_i} \prod_{j=n_1+n_2+1}^{n} e^{\xi_j\theta_j} \boldsymbol{g}_{st,3}(0)\end{aligned}\right\} \tag{1}$$

where $\boldsymbol{g}_{st,2}(\theta) \in \mathbf{R}^{4\times 4}$ and $\boldsymbol{g}_{st,3}(\theta) \in \mathbf{R}^{4\times 4}$ are the final poses of the end-effector of M_2 and M_3 relative to S; $e^{\hat{\xi}_i\theta_i} \in \mathbf{R}^{4\times 4}$ and $e^{\hat{\xi}_j\theta_j} \in \mathbf{R}^{4\times 4}$ are exponential joint twists $\hat{\xi}_i$ and $\hat{\xi}_j$ and respectively, and they represent the rigid motion.

2.2 Inverse kinematics

Based on screw theory and configuration of manipulator, relationship between the joint velocity and the end-effector spatial velocity of M_2 can be described as[8]

$$\dot{\boldsymbol{x}}_2 = \boldsymbol{J}^s_{st,2}\dot{\theta}_2 \tag{2}$$

where

$\dot{\boldsymbol{x}}_2 = (\dot{x}_{1,2} \quad \dot{x}_{2,2} \quad \dot{x}_{3,2} \quad \dot{x}_{4,2} \quad \dot{x}_{5,2} \quad \dot{x}_{6,2})^{\mathrm{T}} \in \mathbf{R}^6$

$\boldsymbol{J}^s_{st,2} = (J_{1,2} \cdots J_{n_1,2} \quad J_{n_1+1,2} \cdots J_{n_1+n_2,2}) \in \mathbf{R}^{6\times(n_1+n_2)}$

$\dot{\theta}_2 = (\dot{\theta}_1 \cdots \dot{\theta}_{n_1} \quad \dot{\theta}_{n_1+1} \cdots \dot{\theta}_{n_1+n_2})^{\mathrm{T}} \in \mathbf{R}^{n_1+n_2}$

$\dot{x}_2$ is the spatial velocity of end-effector of M_2 relative to S; $\boldsymbol{J}^s_{st,2}$ is the spatial Jacobian of M_2; and $\dot{\theta}_2$ is the joint velocity of M_2.

Similar to Eq. (2), the relationship between the joint velocity and the end-effector spatial velocity of M_3 can be described as

$$\dot{\boldsymbol{x}}_3 = \boldsymbol{J}^s_{st,3}\dot{\theta}_3 \tag{3}$$

where

$\dot{\boldsymbol{x}}_3 = (\dot{x}_{1,3} \quad \dot{x}_{2,3} \quad \dot{x}_{3,3} \quad \dot{x}_{4,3} \quad \dot{x}_{5,3} \quad \dot{x}_{6,3})^{\mathrm{T}} \in \mathbf{R}^6$

$\boldsymbol{J}^s_{st,3} = (J_{1,3} \quad \cdots \quad J_{n_1,3} \quad J_{n_1+n_2+1,3} \quad \cdots \quad J_{n,3}) \in \mathbf{R}^{6\times(n_1+n_3)}$

$\dot{\theta}_3 = (\dot{\theta}_1 \quad \cdots \quad \dot{\theta}_{n_1} \quad \dot{\theta}_{n_1+n_2+1} \quad \cdots \quad \dot{\theta}_n)^{\mathrm{T}} \in \mathbf{R}^{n_1+n_3}$

$\dot{\boldsymbol{x}}_3$ is the spatial velocity of end-effector of M_3 relative to S; $\boldsymbol{J}^s_{st,3}$ is the spatial Jacobian of M_3; $\dot{\theta}_3$ is the joint velocity of M_3.

Eqs. (2) and (3) describe the relationship between the joint velocity and the end-effector spatial velocity of M_2 and M_3 respectively. When only M_2 or M_3 performs tasks, Eq. (2) or Eq. (3) can be used to solve the inverse kinematics problem. When M_2 and M_3 perform tasks simultaneously, the inverse kinematics of the manipulator is not simply the sum of the inverse kinematics of M_2 and M_3. Because the first branch is shared by M_2 and M_3, so it is impossible to obtain the correct solutions from the inverse kinematic problem of the manipulator, just simply by summing the solutions of the inverse kinematics problem of M_2 and M_3.

Eq. (2) can be rewritten as

$$\dot{x}_{i,2} = \sum_{j=1}^{n_1} J_{ij,2}\dot{\theta}_j + \sum_{j=n_1+1}^{n_1+n_2} J_{ij,2}\dot{\theta}_j \tag{4}$$

where $\dot{x}_{i,2}$ is the ith element of $\dot{\boldsymbol{x}}_2$; $\dot{\theta}_j$ is the joint velocity of the jth joint; and $J_{ij,2}$ is the ith element of the jth column of $\boldsymbol{J}^s_{st,2}$.

Similarly, Eq. (3) can be rewritten as

$$\dot{x}_{i,3} = \sum_{j=1}^{n_1} J_{ij,3}\dot{\theta}_j + \sum_{j=n_1+n_2+1}^{n} J_{ij,3}\dot{\theta}_j \tag{5}$$

where $\dot{x}_{i,3}$ is the ith element of $\dot{x}_3$; $\dot{\theta}_j$ is the joint velocity of the jth joint; and $J_{ij,3}$ is the ith element of the jth column of $\boldsymbol{J}^s_{st,3}$.

Combining Eqs. (4) and (5), a matrix form equation can be obtained,

$$\dot{\boldsymbol{x}} = \boldsymbol{J}\dot{\theta} = \begin{bmatrix} \boldsymbol{J}^{s}_{st,2} & \boldsymbol{0}_{6\times n_3} \\ \boldsymbol{J}_1 & \boldsymbol{J}_2 \end{bmatrix} \dot{\theta} \qquad (6)$$

where

$\dot{\boldsymbol{x}} = (\dot{x}_{1,2} \quad \cdots \quad \dot{x}_{6,2} \quad \dot{x}_{1,3} \quad \cdots \quad \dot{x}_{6,3})^{\mathrm{T}} \in \mathbf{R}^{12}$

$\dot{\theta} = (\dot{\theta}_1 \quad \dot{\theta}_2 \quad \cdots \quad \dot{\theta}_{n-1} \quad \dot{\theta}_n)^{\mathrm{T}} \in \mathbf{R}^{n}$

$\boldsymbol{J}_1 = (J_{1,3} \quad \cdots \quad J_{n_1,3} \quad \boldsymbol{0}_{6\times n_2}) \in \mathbf{R}^{6\times(n_1+n_2)}$

and

$\boldsymbol{J}_2 = (J_{n_1+n_2+1,3} \quad J_{n_1+n_2+2,3} \quad \cdots \quad J_{n,3}) \in \mathbf{R}^{6\times n_3}$

Eq. (6) can be viewed as the relationship between the joint velocity and the end-effector velocity of serial-typed manipulators. $\dot{\boldsymbol{x}}$ is the end-effector velocity; $\boldsymbol{J}$ is the Jacobian; $\dot{\theta}$ is the joint velocity.

Based on the relationship between the self-motion and Jacobian null space vector[9], the inverse kinematics can be expressed as

$$\left.\begin{aligned} \dot{\theta} &= \boldsymbol{J}^{+}(\theta)\dot{\boldsymbol{x}} + \boldsymbol{J}_{s}\dot{\theta}_{s} \\ \boldsymbol{J}_{s} &= (\boldsymbol{V}_1(\theta) \quad \cdots \quad \boldsymbol{V}_r(\theta)) \end{aligned}\right\} \qquad (7)$$

where $\boldsymbol{J}^{+} \in \mathbf{R}^{n\times 12}$ is the Moore-Penrose inverse Jacobian; $\dot{\theta}_s \in \mathbf{R}^{r}$ is the self-motion velocity; and $\boldsymbol{V}_i(\theta) \in \mathbf{R}^{n}$ is the Jacobian null space vector.

Eq. (7) represents a unified formulation of the trinal-branch space robotic manipulator, which is available for the cooperative manipulation of M_2 and M_3, and the separate manipulation of M_2 or M_3. The former 6 elements of $\dot{\boldsymbol{x}}$ are the end-effector velocities of M_2 and the latter 6 elements are the end-effector velocities of M_3.

3 Simplified Inverse Kinematics of the Trinal-Branch Space Robotic Manipulator

The unified inverse kinematics of the trinal-branch space robotic manipulator is expressed in Eq. (7). Since the dimension of Jacobian is $12\times n$ ($n>12$), the computation of the Moore-Penrose inverse of Jacobian is very complicated. For many real-time applications, Eq. (7) is inapplicable. If each branch features a spherical group of joints at the wrist, a simplified inverse kinematics of the manipulator can be obtained. In this section, the simlified inverse kinematics is discussed.

3.1 Computing the position of the wrist from the pose of end-effector

For the serial-typed manipulator M_2, the pose of the end-effector can be expressed as a 4×4 matrix

$$\begin{bmatrix} n & o & a & p_{\mathrm{end},2} \\ 0 & 0 & 0 & 1 \end{bmatrix}$$

where $p_{\mathrm{end},2} \in \mathbf{R}^{3}$ is the position of the end-effector; n, o, $a \in \mathbf{R}^{3}$ are normal, orientation and approach vectors of the end-effector respectively.

Let $\boldsymbol{P}_{\mathrm{end},2} = (p_{x,2} \quad p_{y,2} \quad p_{z,2})^{\mathrm{T}}$ be the position of the end-effector of M_2 with respect to S; Let $\boldsymbol{P}_{2\mathrm{w}} = (p_{x,2\mathrm{w}} \quad p_{y,2\mathrm{w}} \quad p_{z,2\mathrm{w}})^{\mathrm{T}}$ represents the position of the wrist of M_2 relative to S.

By the definition of the pose of the end-effector, the position of the wrist from the pose of the end-effector can be obtained,

$$\left.\begin{aligned} p_{x,2\mathrm{w}} &= p_{x,2} - L_2\cos\alpha' \\ p_{y,2\mathrm{w}} &= p_{y,2} - L_2\cos\beta' \\ p_{z,2\mathrm{w}} &= p_{z,2} - L_2\cos\gamma' \end{aligned}\right\} \qquad (8)$$

where L_2 is the length of vector $\boldsymbol{P}_{2\mathrm{w}}\boldsymbol{P}_{\mathrm{end},2}$, which is determined by the configuration of the manipulator; γ', β' and α' are the direction angles of vector $\boldsymbol{P}_{2\mathrm{w}}\boldsymbol{P}_{\mathrm{end},2}$ with respect to S.

Similarly, the position of the wrist can be obtained from the pose of the end-effector of M_3.

3.2 Simplified inverse kinematics based on the position control of wrist

Based on the method for Jacobian with screw theory and vector product[9], the relationship between the linear velocity of wrist position and the joint velocity of M_2 can be described as the following map

$$\begin{bmatrix} \dot{p}_{x,2\mathrm{w}} \\ \dot{p}_{y,2\mathrm{w}} \\ \dot{p}_{z,2\mathrm{w}} \end{bmatrix} = [\boldsymbol{J}'_{2\mathrm{w}} \quad \boldsymbol{J}''_{2\mathrm{w}}]\dot{\theta}_{2\mathrm{w}} \qquad (9)$$

where,

$\boldsymbol{J}'_{2\mathrm{w}} = (J_{1,2\mathrm{w}} \quad \cdots \quad J_{n_1,2\mathrm{w}}) \in \mathbf{R}^{3\times n_1}$

$\boldsymbol{J}''_{2\mathrm{w}} = (J_{n_1+1,2\mathrm{w}} \quad \cdots \quad J_{n_1+n_2-3,2\mathrm{w}}) \in \mathbf{R}^{3\times(n_2-3)}$

and

$\dot{\theta}_{2\mathrm{w}} = (\dot{\theta}_1 \quad \cdots \quad \dot{\theta}_{n_1} \quad \dot{\theta}_{n_1+1} \quad \cdots \quad \dot{\theta}_{n_1+n_2-3})^{\mathrm{T}} \in \mathbf{R}^{n_1+n_2-3}$

Similarly, the relationship of the linear velocity of the wrist position and the joint velocity of M_3 can be described as the following map

$$\begin{bmatrix} \dot{p}_{x,3\mathrm{w}} \\ \dot{p}_{y,3\mathrm{w}} \\ \dot{p}_{z,3\mathrm{w}} \end{bmatrix} = [\boldsymbol{J}'_{3\mathrm{w}} \quad \boldsymbol{J}''_{3\mathrm{w}}]\dot{\theta}_{3\mathrm{w}} \tag{10}$$

where

$$\boldsymbol{J}'_{3\mathrm{w}} = (J_{1,3\mathrm{w}} \quad \cdots \quad J_{n_1,3\mathrm{w}}) \in \mathbf{R}^{3\times n_1}$$

$$\boldsymbol{J}''_{3\mathrm{w}} = (J_{n_1+n_2+1,3\mathrm{w}} \quad \cdots \quad J_{n_1+n_2+n_3-3,3\mathrm{w}}) \in \mathbf{R}^{3\times(n_3-3)}$$

and

$$\dot{\theta}_{3\mathrm{w}} = (\dot{\theta}_1 \quad \cdots \quad \dot{\theta}_{n_1} \quad \dot{\theta}_{n_1+n_2+1} \quad \cdots \quad \dot{\theta}_{n-3})^{\mathrm{T}} \in \mathbf{R}^{n_1+n_3-3}$$

Combining Eqs. (9) and (10), a matrix form equation can be obtained

$$\dot{\boldsymbol{x}}_{\mathrm{w}} = \boldsymbol{J}_{\mathrm{w}}\dot{\theta}_{\mathrm{w}} = \begin{bmatrix} \boldsymbol{J}'_{2\mathrm{w}} & \boldsymbol{J}''_{2\mathrm{w}} & \mathbf{0}_{3\times(n_3-3)} \\ \boldsymbol{J}'_{3\mathrm{w}} & \mathbf{0}_{3\times(n_2-3)} & \boldsymbol{J}''_{3\mathrm{w}} \end{bmatrix}\dot{\theta}_{\mathrm{w}} \tag{11}$$

where

$$\dot{\boldsymbol{x}}_{\mathrm{w}} = (\dot{p}_{x,2\mathrm{w}} \quad \dot{p}_{y,2\mathrm{w}} \quad \dot{p}_{z,2\mathrm{w}} \quad \dot{p}_{x,3\mathrm{w}} \quad \dot{p}_{y,3\mathrm{w}} \quad \dot{p}_{z,3\mathrm{w}})^{\mathrm{T}} \in \mathbf{R}^6$$

$$\boldsymbol{J}_{\mathrm{w}} \in \mathbf{R}^{6\times(n-6)}$$

and

$$\dot{\theta}_{\mathrm{w}} = (\dot{\theta}_1 \quad \cdots \quad \dot{\theta}_{n_1+n_2-3} \quad \dot{\theta}_{n_1+n_2+1} \quad \cdots \quad \dot{\theta}_{n-3})^{\mathrm{T}} \in \mathbf{R}^{n-6}$$

Eq. (11) can be viewed as the relationship between the joint velocity and the end-effector velocity of serial-typed manipulator in which the dimensions of work space and joint space are 6 and $n-6$ respectively. $\dot{\boldsymbol{x}}_{\mathrm{w}}$ is the end-effector velocity; $\boldsymbol{J}_{\mathrm{w}}$ is the Jacobian; and $\dot{\theta}_{\mathrm{w}}$ is the joint velocity.

Based on the relationship between the self-motion and the Jacobian null space vector, the inverse kinematics of the position of wrist can be expressed as the following map

$$\left.\begin{aligned} \dot{\theta}_{\mathrm{w}} &= \boldsymbol{J}^{+}_{\mathrm{w}}\dot{\boldsymbol{x}}_{\mathrm{w}} + \boldsymbol{J}_{\mathrm{s,w}}\dot{\theta}_{\mathrm{s,w}} \\ \boldsymbol{J}_{\mathrm{s,w}} &= (\boldsymbol{V}_1(\theta_{\mathrm{w}}) \cdots \boldsymbol{V}_r(\theta_{\mathrm{w}})) \in \mathbf{R}^{(n-6)\times r} \end{aligned}\right\} \tag{12}$$

where $\boldsymbol{J}^{+}_{\mathrm{w}} \in \mathbf{R}^{(n-6)\times 6}$ is the Moore-Penrose inverse of Jacobian; $\dot{\theta}_{\mathrm{s,w}} \in \mathbf{R}^r$ is the self-motion velocity; and $\boldsymbol{V}_i(\theta_{\mathrm{w}}) \in \mathbf{R}^{n-6}$ is the Jacobian null space vector.

3.3 Orientation kinematics of end-effector

Based on Eq. (12), except for joints of wrists of the trinal-branch space robotic manipulator, all the joint velocities can be obtained, and then the joint angles can be obtained by integration.

For M_2, let $\boldsymbol{R}_{\mathrm{end},2}$ be the desired orientation of the end-effector. Let $\boldsymbol{R}_{2\mathrm{w}}$ represent the final orientation of the wrist which can be calculated by using forward kinematics. One can be obtained

$$\boldsymbol{R}_{2\mathrm{w}} \times \mathrm{Euler}(\theta_{n_1+n_2-2} \quad \theta_{n_1+n_2-1} \quad \theta_{n_1+n_2}) = \boldsymbol{R}_{\mathrm{end},2} \tag{13}$$

where $\mathrm{Euler}(\theta_{n_1+n_2-2} \quad \theta_{n_1+n_2-1} \quad \theta_{n_1+n_2})$ is the Euler transformation of the last three joints in the wrist of M_2.

Then, the following can be gotten:

$$\mathrm{Euler}(\theta_{n_1+n_2-2} \quad \theta_{n_1+n_2-1} \quad \theta_{n_1+n_2}) = (\boldsymbol{R}_{2\mathrm{w}})^{-1}\boldsymbol{R}_{\mathrm{end},2} \tag{14}$$

By solving Eq. (14), $\theta_{n_1+n_2-2}$, $\theta_{n_1+n_2-1}$ and $\theta_{n_1+n_2}$ can be obtained.

Similarly, for M_3, one can be obtained

$$\mathrm{Euler}(\theta_{n-2} \quad \theta_{n-1} \quad \theta_n) = (\boldsymbol{R}_{3\mathrm{w}})^{-1}\boldsymbol{R}_{\mathrm{end},3} \tag{15}$$

where $\boldsymbol{R}_{\mathrm{end},3}$ is the desired orientation of the end-effector of M_3; and $\boldsymbol{R}_{3\mathrm{w}}$ is the final orientation of the wrist which can be calculated by using forward kinematics.

Therefore, using Eqs. (11), (14) and (15), the solutions of the inverse kinematics problem of the trinal-branch space robotic manipulator can be obtained. The kinematics algorithm reduces the dimension of the Moore-Penrose inverse Jacobian from $n \times 6$ to $(n-6) \times 6$. Thus, it reduces the computation of solving the inverse kinematics problem.

4 Simulation

To illustrate the inverse kinematics proposed by this paper, a trinal-branch space robotic manipulator will be discussed in this section, as shown in Fig. 2. Each branch has 5 revolute joint and features a spherical group of joints at the wrist, and the configuration and dimension of each branch are shown in Fig. 2(b). The trinal-branch manipulator is mounted on a guide track with one degree, as shown in Fig. 2(a). Thus, there are 16 degrees of freedom totally in this system.

Fig. 3 shows the trinal-branch space robotic manipulator in its zero-reference-position. The coordinate system is shown in Fig. 4 in its zero-reference-position, and the twist coordinates of each joint are given by

$$\xi_0=(0\quad 1\quad 0\quad 0\quad 0\quad 0)^{\mathrm{T}}$$
$$\xi_1=(0\quad 0\quad 0\quad 0\quad 0\quad 1)^{\mathrm{T}}$$
$$\xi_2=(0\quad 0.2\quad 0\quad 1\quad 0\quad 0)^{\mathrm{T}}$$
$$\xi_3=(0\quad 0\quad 0\quad 0\quad 0\quad 1)^{\mathrm{T}}$$
$$\xi_4=(-0.59\quad 0\quad 0\quad 0\quad 1\quad 0)^{\mathrm{T}}$$
$$\xi_5=(0\quad 0.83\quad 0.1\quad 1\quad 0\quad 0)^{\mathrm{T}}$$
$$\xi_6=(0\quad 1.21\quad 0.1\quad 1\quad 0\quad 0)^{\mathrm{T}}$$
$$\xi_7=(-1.45\quad 0\quad 0\quad 0\quad 1\quad 0)^{\mathrm{T}}$$
$$\xi_8=(-0.2\quad 0\quad 0\quad 0\quad 0\quad 1)^{\mathrm{T}}$$
$$\xi_9=(0\quad 1.84\quad 0.2\quad 1\quad 0\quad 0)^{\mathrm{T}}$$
$$\xi_{10}=(-0.2\quad 0\quad 0\quad 0\quad 0\quad 1)^{\mathrm{T}}$$
$$\xi_{11}=(0\quad 1.02\quad 0.43\quad 1\quad 0\quad 0)^{\mathrm{T}}$$
$$\xi_{12}=(-0.67\quad 0\quad 0\quad 0\quad 0\quad 1)^{\mathrm{T}}$$
$$\xi_{13}=(0.92\quad 0\quad 0\quad 0\quad -1\quad 0)^{\mathrm{T}}$$
$$\xi_{14}=(-1.06\quad 0\quad 0\quad 1\quad 0\quad 0)^{\mathrm{T}}$$
$$\xi_{15}=(0.92\quad 0\quad 0\quad 0\quad -1\quad 0)^{\mathrm{T}}$$

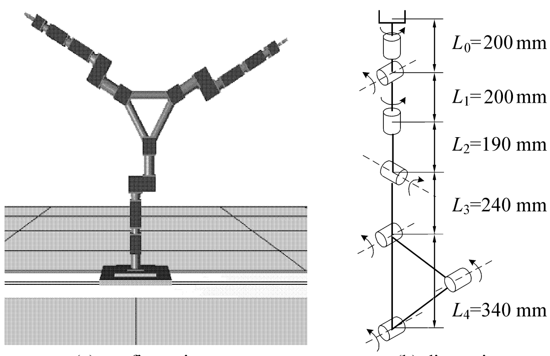

(a) configuration (b) dimension

Fig. 2 A trinal-branch space robotic manipulator

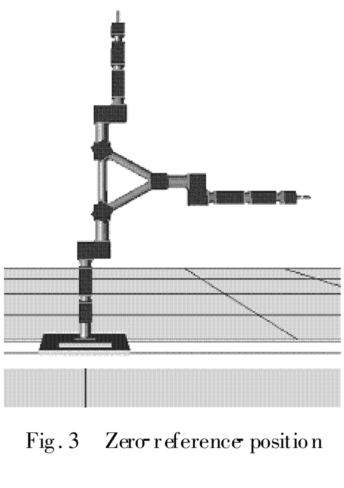

Fig. 3 Zero-reference-position

Fig. 5(a) shows the initial state of the manipulator at the beginning of the simulation. At this time, the poses of the end-effectors of M_2 and M_3 are given by

$$\boldsymbol{g}_{\mathrm{st},2}=\begin{bmatrix}1 & 0 & 0 & 0\\ 0 & 1/2 & \sqrt{3}/2 & 0.76\\ 0 & -\sqrt{3}/2 & 1/2 & 1.66\\ 0 & 0 & 0 & 1\end{bmatrix}$$

$$\boldsymbol{g}_{\mathrm{st},3}=\begin{bmatrix}1 & 0 & 0 & 0\\ 0 & 1/2 & -\sqrt{3}/2 & -1.06\\ 0 & \sqrt{3}/2 & 1/2 & 1.49\\ 0 & 0 & 0 & 1\end{bmatrix}$$

First, M_2 is driven to open the door of the cabinet; and then M_3 is operated to take a bolt out the cabinet simultaneously; finally M_2 is manipulated to close the door of cabinet.

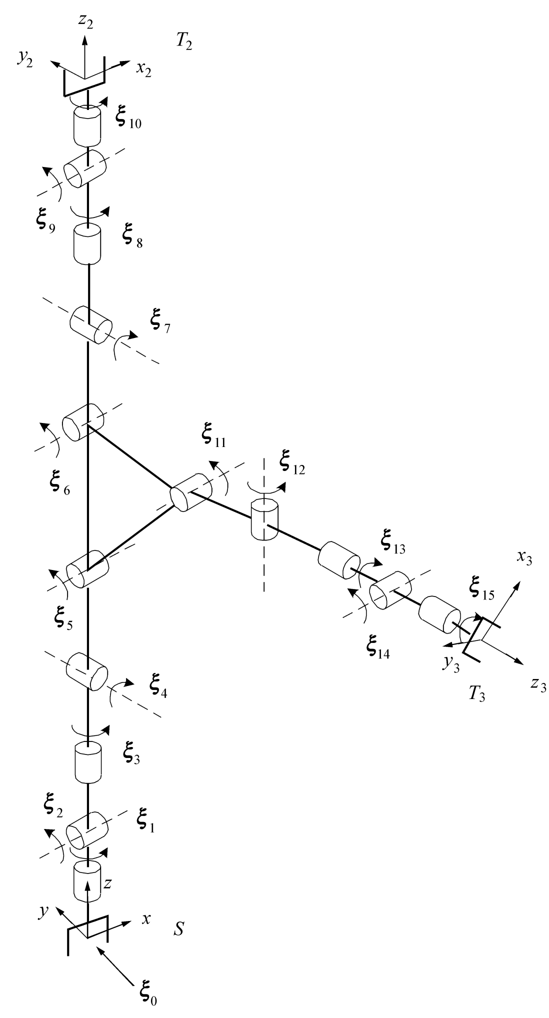

Fig. 4 Coordinate system

The simulation time is 20 s. Fig. 5(b), 5(c), 5(d), 5(e) and 5(f) show the configuration of the manipulator in t = 4.0 s, 8.0 s, 12.0 s, 16.0 s and 20.0 s respectively.

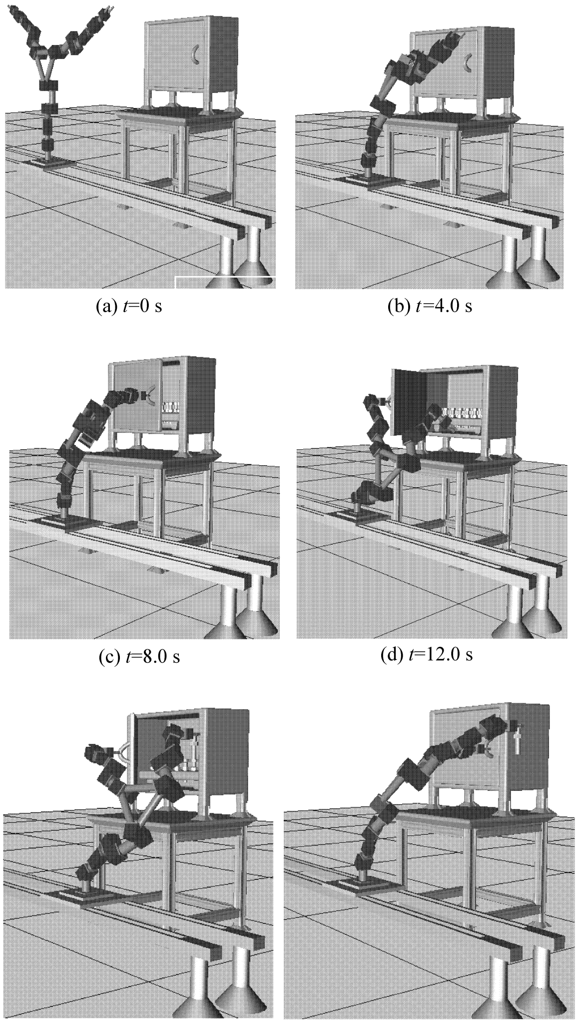

(a) t=0 s (b) t=4.0 s (c) t=8.0 s (d) t=12.0 s (e) t=16.0 s (f) t=20.0 s

Fig. 5 Movements of the trinal-arm manipulator

5 Conclusions

A trinal-branch space robotic manipulator with redundancy due to the harsh application environments is introduced. The inverse kinematics problem of the trinal-branch space robotic manipulator is investigated, and its unified formulation is established. That simplified inverse kinematics for each branch features a spherical group of joints is proposed. The inverse kinematic algorithm reduces the dimension of Moore-Penrose inverse of Jacobian from $n \times 6$ to $(n-6) \times 6$. Thus, it reduces the computation through solving the inverse kinematics problem. Finally, its feasibility is demonstrated by the computer simulation results.

References

[1] Hirzinger G, Brunner B, Dietrich J, *et al*. ROTEX-the first remotely controlled robot in space[A]. Proc of IEEE Int Conf on Robotics and Automation[C]. CA USA, 1994. 2604-2611.

[2] Matsueda T, Kuraoka K, Goma K, *et al*. JEMRMS system design and development status[A]. Proc of Telesystems Conference[C]. GA USA, 1991. 391-395.

[3] Xu Y S, Brown H B. Control system of the self-motion space manipulator[J]. IEEE Transaction on Control Systems Technology, 1994, 2(3): 207-219.

[4] http://ranier.hq.nasa.gov/telerobotics_page/FY96Plan/Chap2h.html

[5] Ren J Y. Technology research on multi-axis, multi-arm space robot[D]. Beijing: Beijing University of Aeronautics and Astronautics, 2001.

[6] Lewis L, Maciejewski A. Fault tolerant operation of kinematically redundant manipulators for locked joint failures[J]. IEEE Transaction on Robotics and Automation, 1997, 13(4): 621-629.

[7] Denavit J, Hartenberg R S. A kinemtic notation for lower pair mechanisms based on matrice[J]. Applied Mechanics, 1995, 22: 215-221.

[8] Murray R, Li Z, Sastry S S. A mathematical introduction to robotic manipulation [M]. Boca Raton, FL: CRC Press, 1994.

[9] Zhou D H. On the mechanism study of redundant robots[D]. Beijing: Beijing University of Aeronautics and Astronautics, 1994.

Biographies:

JIA Qing-xuan (1964-) male, born in Shandong. He is a doctoral candidate in Beijing University of Aeronautics and Astronautics. And he is a professor in the automation school at Beijing University. of Posts and Telecommunications. His research interests include the mechanical design, robot and virtual reality.

Tel: 010-62286776, E-mail: sdjqx@sohu.com